RESONANCE LAMP ABSORPTION MEASUREMENT OF OH NUMBER DENSITY AND TEMPERATURE IN EXPANSION TUBE SCRAMJET ENGINE TESTS*

Walter R. Lempert
Dept. of Mechanical & Aerospace Engineering
Princeton University
Princeton, New Jersey

Richard E. Trucco
General Applied Science Laboratories
Ronkonkoma, New York

Robert D. Bittner
Analytical Services and Materials, Inc.
Hampton, Virginia

INTRODUCTION

Optical absorption techniques have been used to obtain quantitative flow field and species data in a variety of combustion environments. Hanson and his co-workers (1) have developed an ultraviolet rapid (KHz) scanning method employing the second harmonic from a modified commercial ring dye laser which has been used to measure hydroxyl radical (OH) and nitric oxide (NO) (2) concentrations, as well as static temperature, density, and flow velocity. Recently, Cavolowsky, et al., (3) have applied this approach to the NASA-Ames 16-inch hypersonic shock tunnel, obtaining hydroxyl number density and static temperature. Frequency Modulation (FM) techniques have also been demonstrated for water vapor (4) and oxygen (5).

In this paper, we report results of hydroxyl radical and static temperature measurements performed in the General Applied Science Laboratories-NASA HYPULSE expansion tube facility using the microwave resonance lamp absorption technique (6,7,8). Data were obtained as part of a series of hydrogen/air and hydrogen/oxygen combustion tests at stagnation enthalpies corresponding to Mach 17 flight speeds. Data from a representative injector configuration is compared to a full Navier-Stokes CFD solution.

TEST FACILITY

Testing for this study was conducted in the GASL/NASA HYPULSE facility, isometrically portrayed in Fig. 1. HYPULSE, a 6-inch diameter, 115-ft long expansion tube, was built by NASA-Langley Research Center in the late 1960's, and decommissioned in 1983. In October 1987, the facility was transferred to GASL, and by May 1989, the full NASA operating capability was recovered. The operation of the expansion tube is similar to that of two shock tubes in series.

* Work done on contract at General Applied Sciences Laboratories, NAS1-18450.

The driver section initiates the test flow in the first (intermediate) tube, which in turn starts the flow in the second (acceleration) tube, accelerating the flow to velocities necessary for hypersonic flight simulation by means of an unsteady expansion. These two sections are separated by a thin mylar diaphragm. The distance-time (x,t) diagram of Fig. 2 illustrates ideal expansion tube flow, where the shaded region represents the test gas. A complete description of the operation of the expansion tube is given in References 9-11. The critical feature of this facility is the ability to generate high enthalpy flow without stagnation. This results in low levels of dissociated nonequilibrium species, and, therefore, more closely resembles real free stream flight conditions. The tradeoff for this benefit is the brevity of the test time, nominally 250 to 400 microseconds.

The facility test conditions, derived from a combination of measured in-stream pitot and static pressures, wall static pressure and shock arrival speed, are shown in Table I. From these measurements, the quantities of Table II are calculated applying the numerical procedures described in Reference 12. A full description of the experimental efforts to calibrate the HYPULSE facility is detailed in Reference 13.

COMBUSTOR MODEL

Figure 3 shows a schematic of the combustor model utilized for the test series, configured with a 15° flush wall fuel injector. The constant area model is 2" x 1" in cross section, 28" long and located so that its inlet is 1" from the exit of the acceleration tube. The leading edges are sharp wedges with a nominal tip bluntness of 0.020" diameter. Flow visualization of the near-field fuel injection region is afforded by 12" side windows (either BK-7 or fused silica glass). One-inch diameter UV windows, located at 17" and 26" from the inlet provide line-of-sight visibility for the OH absorption measurements. Access for planar laser fluorescence imaging, described in a separate paper (14), was achieved through a 6.25" x 1.125" fused silica window on the upper wall. The assembled model is shown in Fig. 4.

Interchangeable fuel injection manifold plates, located on the upper and lower walls at 6" from the inlet, are fed by the injector plenum. The injectors used during these tests were: A 15° flush wall injector, a single-hole 10° dual-swept ramp injector, and a 10° single unswept ramp injector. Hydrogen fuel was supplied to the unswept plenum by a Ludwig tube mechanism opened to synchronize with the test flow by fast acting valves as described in Reference 15.

The model was fitted with an array of piezoelectric pressure transducers and specially designed thin-film heat flux gauges, located throughout the upper and lower walls.

OH RESONANCE ABSORPTION METHOD

The resonance lamp absorption technique, illustrated schematically in Fig. 5, is described in detail in References 6-8 and will only be summarized here. A low pressure water vapor microwave discharge provides a source of narrow bandwidth, ultraviolet emission lines from the hydroxyl radical X-A band near 309 nm. In the current experiments, the lamp output was amplitude modulated at 23 KHz using a 150 sector chopper wheel and coupled into UV transmitting optical fiber which "pipes" the light to the expansion tube. A lens is used to collimate the light through the combustor in an approximately 1/2" diameter beam. A second lens couples the partially transmitted beam into a receiving fiber to a custom polychrometer. The polychrometer consists of a fiber optic bundle placed in the exit plane of a 0.25 m spectrometer which disperses the OH A-X emission into eight spectral channels of approximately 1.50 nm width.

Individual phototubes are used to obtain the absorption in each spectral channel as a function of time. The analogue bandwidth was adjusted to approximately 100 KHz with a 5 Kohm parallel load resistor. Each channel was digitized with a LeCroy model 6810 A/D converter. The experimental absorption in each channel was averaged over the approximately 200 microsecond steady-state run time, yielding a single set of temporally and spatially averaged absorption values which is inverted to yield OH number density and static temperature.

As described in References 6-8, the lamp emission consists of approximately 100 discrete rotational transitions from both the (0,0) and (1,1) vibrational bands, resulting in a hybrid rotational/vibrational temperature determination.

FACILITY INTERFACE

Figure 6 shows the resonance lamp absorption apparatus, as assembled for the HYPULSE combustion tests. The lamp, chopper wheel, polychrometer, and associated power supplies and gauges were mounted on a 2' x 4' optical breadboard, located in a room adjacent to the expansion tube. The lamp output was transmitted to the facility with a 5 meter length of 1100 micron core silica fiber. The feed-thru to the test chamber was accomplished with a 1.5" length of 0.3125" OD x 0.047" ID tubing in the following manner: First the protective jacket was spliced and removed over half the length of the fiber. The bare core and cladding were then slid through the 0.047" ID tube, and sealed on both ends with silicon adhesive. This resulted in a leak proof feed-thru, without requiring a break in the fiber. The protective jacket was then replaced. The portion of the fiber inside the test chamber was threaded through rubber hoses to the collimating lens assembly to provide additional protection from post-test stresses. Threaded tubing, secured to the model side wall, fixed the optics and provided a pressure seal. The windows were 1" diameter with an additional 0.25" lip for flush mounting with the model inside surface. Despite these precautions, facility stresses did cause occasional damage to the windows, requiring replacement. Post-flow contamination from the secondary mylar diaphragm attenuated the transmission by approximately 30%, necessitating periodic cleaning. Figure 7 shows a schematic of the optical fiber/model interface, and Fig. 8 shows the assembly inside the test section.

ONE-DIMENSIONAL ABSORPTION MODELING

The inversion of the experimental data is performed by means of a discrete least-squares fit to a surface of transmission values generated using a standard spectral model which is described in detail in Reference 8. The surface consists of 8 transmission values for each point in a 49 x 31 grid of OH number density-path length product, Nl, and static temperature. The Nl grid runs from 1.0×10^{15} cm^{-2} to 1.0×10^{18} cm^{-2} in factors of $10^{.0625} = (1.15)$, and the temperature grid runs from 1000 to 4000 K in 100 K increments. The result of the inversion procedure is a one-dimensional value of OH number density and static temperature, averaged spatially over the beam path and beam dimensions.

RESULTS

The application of the technique to the HYPULSE expansion tube presented a significant challenge due to the severe environment and short (<300 microsecond) run times. Despite the fact that the measurements were performed 26" downstream from the model leading edge, where,

presumably, combustion was no longer occurring, the signal due to spontaneous combustor luminosity was as large, or larger, than that from the lamp itself. This, coupled with the high analogue bandwidth required to perform the measurement, resulted in lower signal-to-noise than obtained in previous experiments (7,8). In addition, for some tests the OH number density and static temperature were sufficiently high to cause virtually complete absorption, resulting in data which could not be inverted. Nonetheless, useful data was obtained for a ϕ = 1 (based on air), 15° flush wall injector H_2/O_2 test, and a ϕ = 3, 10° dual-swept ramp injector H_2/air test. Figure 9 shows the experimental time trace from spectral channels 2 and 7 for a 15° flush wall injector ϕ = 1--H_2/O_2 combustion run. The run starts at approximately 5.18 msec. The stable run time, for which the data was averaged, is from 5.40 to 5.55 msec. The experimental transmission values are 0.16 ± 0.02, and 0.68 ± 0.05 for channels 2 and 7, respectively.

Table III shows the experimental transmission values for the two tests described below. Also shown is the corresponding one-dimensional values for OH number density and static temperature, and an estimate of their uncertainty. (Due to limitations on the available number of facility A/D channels, spectral channels which had the lowest signal-to-noise ratio were not recorded.) The mean values and uncertainty estimates are obtained by performing the data inversion for all 729 (3^6) possible combinations of measured transmission values ± the uncertainty in the measured transmission. The results represent the mean and RMS deviation from the procedure. (It should be stressed that these are statistical uncertainties based upon the observed signal-to-noise ratio in the experimental data.) While it is difficult to compare these two tests due to differences in injectors, equivalence ratio, and mixture, it is not unrealistic to conclude that the H_2/O_2 test would be expected to result in higher OH number density than the H_2/air test.

COMPARISON TO CFD

A full Navier-Stokes CFD solution was performed for the 15 degree flush wall injection, ϕ = 1.0 test described above. Figures 10 and 11 show contour plots of average OH number density and static temperatures as a function of height above the bottom wall (Z-axis), integrated in the lateral dimension (Y-axis). Also shown is the lamp output beam dimension and position. The variation with respect to the flow direction (X-axis) is considerably less. While there is no direct way to compare the experimental 1D absorption data with the CFD prediction, an analysis was performed as follows: First, a computer code was written to simulate the experimental absorption expected from a flow described by the CFD grid. This required spatial integration of the absorption in both the Z and Y dimensions. This integration was performed differently in the two dimensions. In Z (vertical), the CFD values for both OH number density and temperature were <u>averaged</u> over the beam height. This average was weighted to reflect the circular cross section of the beam, assuming negligible X (flow axis) dependence over the diameter of the beam (1/2"). This weighted averaging resulted in a single value of OH and T for each Y grid point. The absorption coefficients, $K_y(N)$, for each of the N spectral channels were then calculated using these OH and T values for each of the Y grid points. The simulated transmission in each channel is given by:

$$\tau_N = \sum_y \exp\left[-(K_y(N)\, l_y\right] \qquad (1)$$

where l_y is the length in the y direction of the "yth" grid element. (Note that the CFD grid is <u>not</u> equally spaced.) The final result of this procedure is a set of eight transmission values which are listed in Table IV. Comparison of Tables III and IV shows that the results of this

simulation predict transmission values which are on the order of 30 to 40% lower than the experimental data.

In order to attempt a more tangible assessment of the comparison between the CFD prediction and the experimental data, a sensitivity analysis was performed. This was done by repeating the above simulation procedure for all 9 combinations of CFD grid values ±40% for OH and ±10% for temperature. Table V shows the resulting 9 sets of simulated transmission values. Comparison of Tables III and V indicates that modification of the CFD predictions for OH by ±40% and T by ±10% result in a range of transmission values which bracket the experimental data to within the estimated statistical uncertainty.

As a final comparison, the simulated transmission values from the CFD grid were "inverted" with the 1D software to obtain 1D equivalent OH density and temperature. The resulting OH number density is 4.27×10^{16} cm^{-3} and resulting static temperature is 2606 K. Comparison with the data of Table III indicates a discrepancy of approximately 40% in OH number density, and 10% in static temperature. There are several possible sources of error. First, a detailed measurement of the size of the beam as a function of lateral position (Y) was not performed. In general, the collimation of the 1100 micron core fiber is far from perfect, resulting in a beam size which varies with position. Second, the beam is assumed to have a uniformly intense circular cross section, which is clearly not the case. Finally, it is difficult to accurately predict the free stream inlet conditions produced by the expansion tubes. Calibrations performed just prior to the test sequence resulted in a measured static pressure and temperature of 14,478 Pa and 2237 K, respectively. The nominal values assumed for the CFD calculation were 16,478 Pa and 2089 K, respectively.

In attempting to assess the significance of the resonance absorption results with respect to CFD validation, it is useful to compare the above 1D equivalent results for OH and T with spatial averages of the CFD grid itself. A simple linear averaging of the contours of Figs. 10 and 11 over the beam profile results in $OH_{ave} = 4.26 \times 10^{16}$ cm^{-3} and $T_{ave} = 3037$ K. The level of agreement between average OH and equivalent 1D OH is actually surprising considering the highly two-dimensional character of the flow field and the nonlinear nature of the absorption process. The discrepancy in temperature is most likely due to the inverse correlation of OH density and static temperature. From Figs. 10 and 11 it can be seen that the CFD predicts relatively low temperatures in regions of relatively high OH. Since the integral transmission is weighted by the regions of high OH Density, the result is a low value for 1D equivalent temperature.

From the above it is fair to conclude that, for this case, the experimental resonance absorption OH concentration and static temperature are expected to agree within the order of 10% with the spatially averaged results of the CFD calculation, in the absence of any additional systematic error. Additional sets of data and calculations will be required in order to determine the generality of this statement for three-dimensional reacting flow fields.

CONCLUSIONS

The resonance lamp absorption method has been used to obtain temporally averaged line-of-sight static temperature and OH concentrations in the HYPULSE hypersonic expansion tube facility. A comparison of the experimental data with a full CFD solution has been performed for a 15° flush wall injector, H_2/O_2 combustion configuration. The experimentally determined OH number density was approximately 40% below the simulated prediction using the CFD grid, while experimental static temperature was approximately 10% low. It is likely that some of this discrepancy is due to the nominal combustor inlet density used for the CFD, which was

approximately 20% higher than that actually produced by the facility. Comparison of simulated temperature and OH number density, with simple spatial averaging of the CFD grid, resulted in agreement to within approximately 10%.

ACKNOWLEDGEMENTS

The authors wish to acknowledge R. Gregory for providing the resonance lamp absorption instrumentation, and C. Rogers, R. McClinton, and J. Erdos for useful discussions.

REFERENCES

1. Davidson, D.F., Chang, A.Y., DiRosa, M.D, and Hanson, R.K., "Continuous Wave Laser Absorption Techniques for Gasdynamic Measurements in Supersonic Flows," Appl. Opt. 30, p. 2598 (1991).

2. Chang, A.Y., DiRosa, M.D., Davidson, D.F., and Hanson, R.K., "Rapid Tuning cw Laser Technique for Measurements of Gas Velocity, Temperature, Pressure, Density, and Mass Flux Using NO," Appl. Opt. 30, p. 3011 (1991).

3. Cavolowsky, J. and Newfield, M., "Laser Absorption Measurements of OH Concentration and Temperature in Pulsed Facilities," AIAA 92-0142, 30th Aerospace Sciences Meeting, Reno, NV, January 6-9, (1992).

4. Wang, L-Q, Riris, H., Carlisle, C.B., and Gallagher, T.F., "Comparison of Approaches to Modulation Spectroscopy with GaAlAs Semiconductor Lasers: Application to Water Vapor," Appl. Opt. 27, p. 2071 (1988).

5. Philippe, L. and Hanson, R., AIAA-92-0139, "Sensitive Diode Laser Absorption Technique for Aerodynamic Measurements," 30th Aerospace Sciences Meeting, Reno, NV, January 6-9 (1992).

6. Lempert, W.R., "Microwave Resonance Lamp Absorption Technique for Measuring Temperature and OH Number Density in Combustion Environments," Combustion and Flame 73, p. 89 (1988).

7. McCullough, R.W. and Northam, G.B., in "Temperature, Its Measurement and Control in Science and Industry," J.F. Schooley, Editor, American Institute of Physics, New York, p. 665, Vol. 5, Pt. 1 (1982).

8. Northam, G.B., Lempert, W.R., Diskin, G.S., Gregory, R.W., and Bell, R.A., "Supersonic Combustion Performance of Hydrogen/Hydrocarbon Mixtures as Determined by a Nonintrusive Temperature Monitor," AIAA-88-3293, AIAA/SAE/ASME/ASEE 24th Joint Propulsion Conference, Boston, MA, July 11-13 (1988).

9. Miller, C.G., and Jones, J.J., "Development and Performance of the NASA-Langley Research Center Expansion Tube/Tunnel, a Hypersonic-Hypervelocity Real Gas Facility," 14th International Symposium on Shock Tubes and Waves, Sydney, Australia, August 15-18, 1983.

10. Tamagno, J., Bakos, R.J., and Pulsenetti, M.V., "Results of Preliminary Calibration Test in the GASL HYPULSE facility," NASP Contractor Report 1071, Ref. WBS 2.2.21, November 1983.

11. Tamagno, J., Bakos, R.J. Pulsenetti, M.V., and Erdos, J., "Hypervelocity Real Gas Capabilities of GASL's Expansion Tube (HYPULSE) Facility," AIAA Paper No. 90-1390, June 1990.

12. Mirels, H., "Test Time in Low-Pressure Shock Tubes," Physics of Fluid 6 (9), September 1963.

13. Calleja, J., and Tamagno, J., "Calibration of HYPULSE for Hypervelocity Air Flows Corresponding to Flight Mach Numbers 13.5, 15, and 17"," GASL TR 335, February 1992.

14. Rubin, L.F., Swain, D.M., and Trucco, R.E., "Visualization of Hydrogen Injection in a Scramjet Engine by Simultaneous Planar Laser-Induced Fluorescence Imaging and Laser Holographic Interferometry," Proceedings of the NASA Langley Measurement Technology Conference, Hampton, VA, NASA CP-3161, 1992.

15. Trucco, R., and Danziger, L., "Performance of a Fast-Acting Valve for Hydrogen Injection into a SCRAMJET Engine Model," GASL TM 232, September 1989.

TABLE I. HYPULSE Calibration Data--Measured Quantities

Nominal Conditions	M13.5 LP	M13.5 HP	M15	M17	M17 with Diffuser Air	M17 with Diffuser Oxygen
Driver Pressure (MPa)	37.9	51.7	37.9	37.9	37.9	37.9
Static Pressure (KPa)	18.0 ± 0.3	23 ± 1	1.52 ±.07	2.00 ± 0.07	16 ± 2	14.5 ± 2
Core Pitot Pressure (KPa)	386 ± 32	510 ± 47	105 ± 6	156 ± 9	663 ± 90	602 ± 85
Secondary Shock Speed (M/S)	4169 ± 24	4176 ± 30	4707 ± 19	5176 ± 42	5244 ± 42	5189 ± 40
Useful Test Time (Microseconds)	450	450	400	350	350	350

TABLE II. HYPULSE Calibration Data--Calculated Quantities

Nominal Conditions	M13.5 LP	M13.5 HP	M15	M17	M17 with Diffuser Air	M17 with Diffuser Oxygen
Total Enthalpy (MJoule/kg)	9.89	9.84	11.14	14.05	15.07	16.16
Total Pressure (MPa)	10.3	14.7	59.8	153.1	138.0	258.0
Total Temperature (^{o}K)	5780	5830	6870	8070	8370	6980
Static Temperature (^{o}K)	2350	2280	1050	1140	2100	2240
Velocity (M/S)	3840	3840	4630	5120	5090	4960
Mach Number	4.10	4.19	7.31	7.77	5.75	5.75

TABLE III. Experimental Results from OH Resonance Absorption Measurements in HYPULSE Combustion Experiments

15 Degree Flush Wall Injector -- ϕ = 1.0, H_2/O_2

	1	2	3	4	5	6	7	8
Tau	0.18	0.16	0.16	0.26	--	0.59	0.68	--
Sig Tau	0.03	0.02	0.03	0.05	--	0.08	0.05	--

Mean OH Number Density: 2.7×10^{16} cm^{-3}
Statistical Uncertainty: 2.7×10^{15} cm^{-3}
Mean Static Temperature: 2320 K
Statistical Uncertainty: 204 K

10 Degree Dual-Swept Ramp Injector -- ϕ = 3.0, H_2/air

	1	2	3	4	5	6	7	8
Tau	0.39	0.27	0.36	0.52	--	--	0.7	--
Sig Tau	0.05	0.03	0.04	0.04	--	--	0.04	--

Mean OH Number Density: 1.2×10^{16} cm^{-3}
Statistical Uncertainty: 9.9×10^{14} cm^{-3}
Mean Static Temperature: 2320 K
Statistical Uncertainty: 322 K

TABLE IV. Simulation of ID OH Transmission from CFD Grid

15 Degree Flush Wall Injection -- ϕ = 1.0

H_2/O_2

26" Downstream from Leading Edge

	1	2	3	4	5	6	7	8
Tau	0.146	0.094	0.096	0.143	0.323	0.439	0.535	0.618

TABLE V. Sensitivity Analysis Results from CFD Solution

TAU VALUES

OH/<OH>	T/<T>	1	2	3	4	5	6	7	8
0.60	0.90	.25	.13	.15	.22	.46	.60	.70	.77
0.60	1.00	.27	.15	.17	.23	.44	.57	.66	.74
0.60	1.10	.29	.16	.19	.23	.43	.56	.65	.72
1.00	0.90	.13	.08	.08	.14	.35	.48	.58	.66
1.00	1.00	.15	.09	.10	.14	.32	.44	.53	.62
1.00	1.10	.16	.10	.11	.14	.31	.42	.51	.59
1.4	0.90	.08	.06	.06	.11	.28	.39	.49	.58
1.4	1.00	.09	.07	.07	.11	.26	.35	.44	.53
1.4	1.10	.10	.07	.07	.11	.25	.33	.42	.50

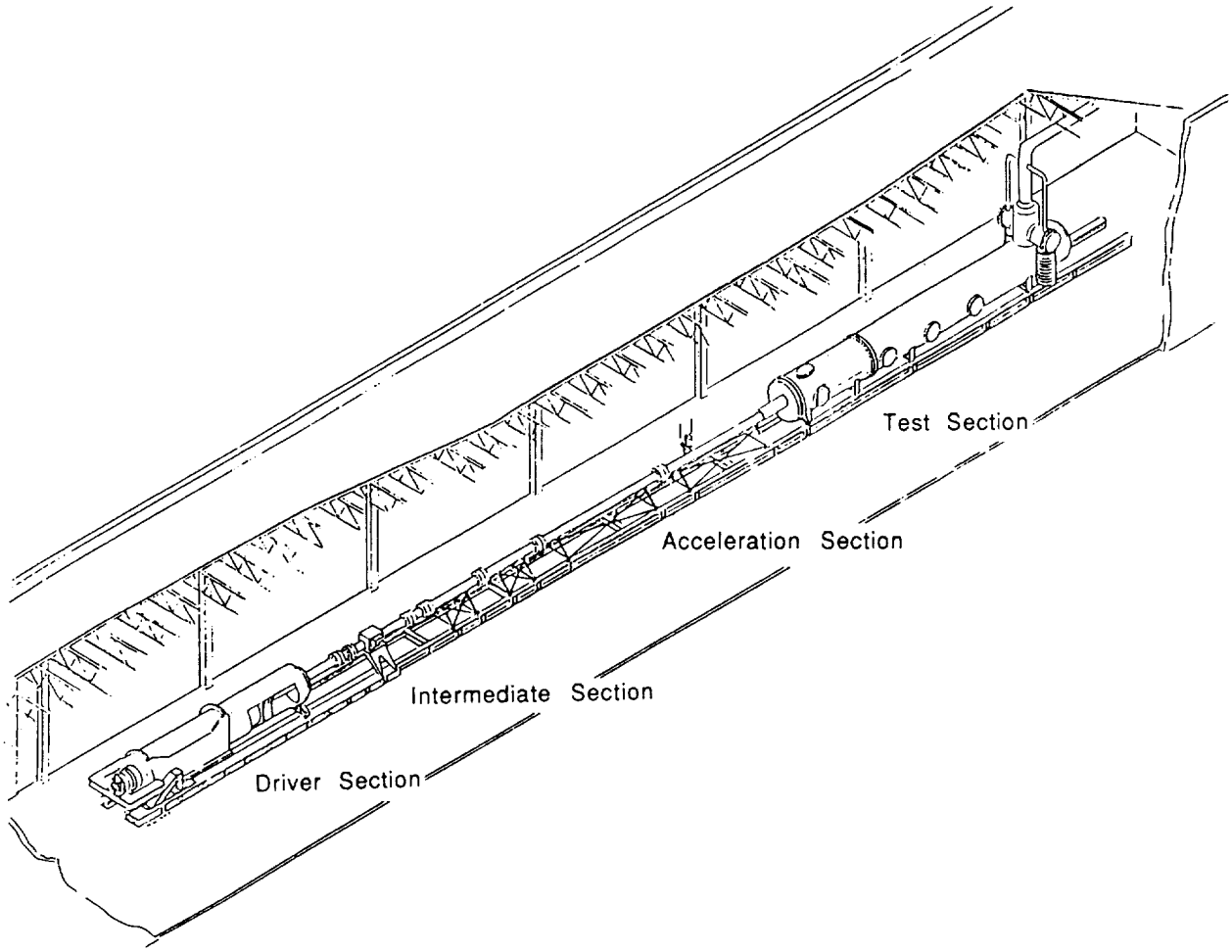

Figure 1. Isometric view of HYPULSE expansion tube.

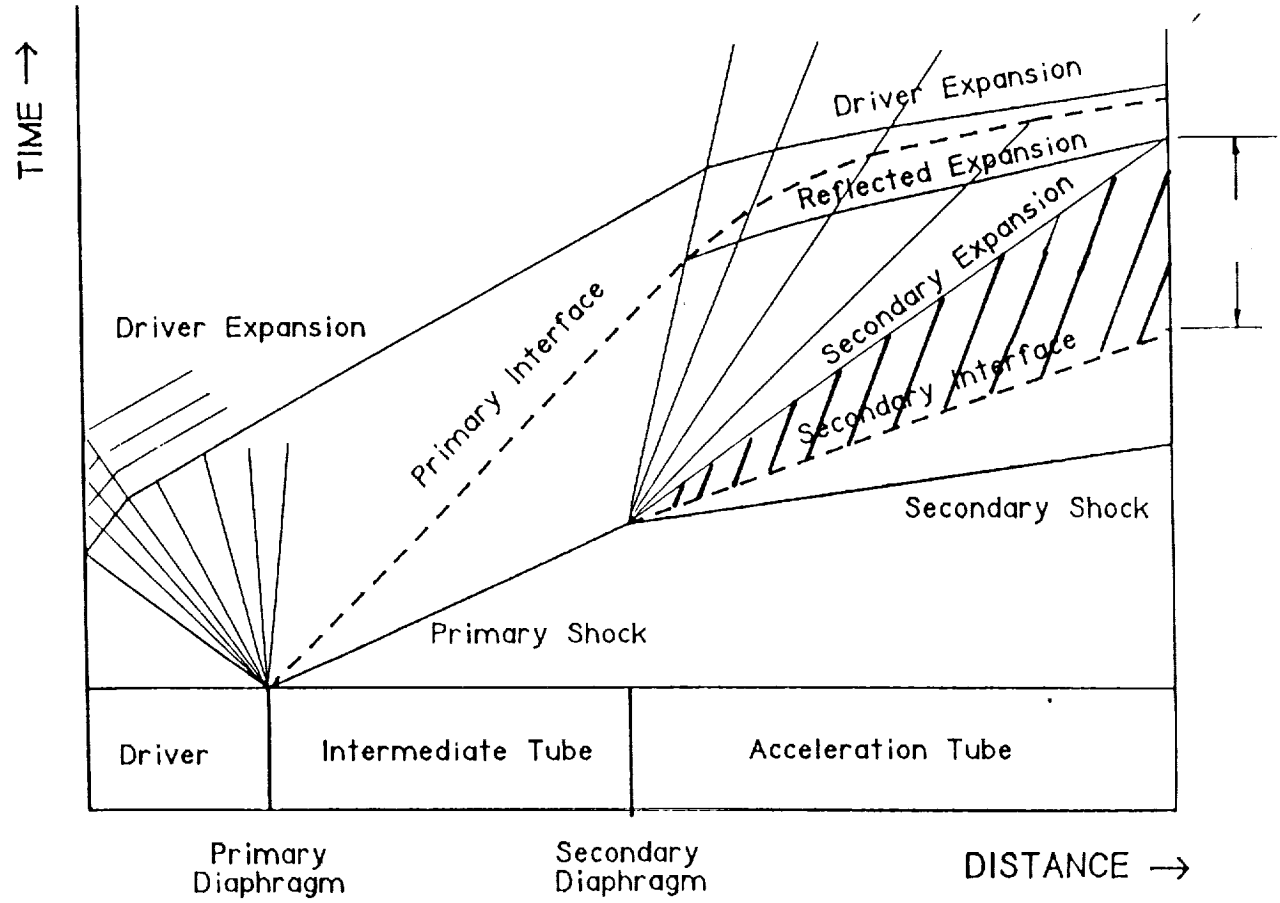

Figure 2. Time-distance for ideal expansion tube. Shaded region represents test gas.

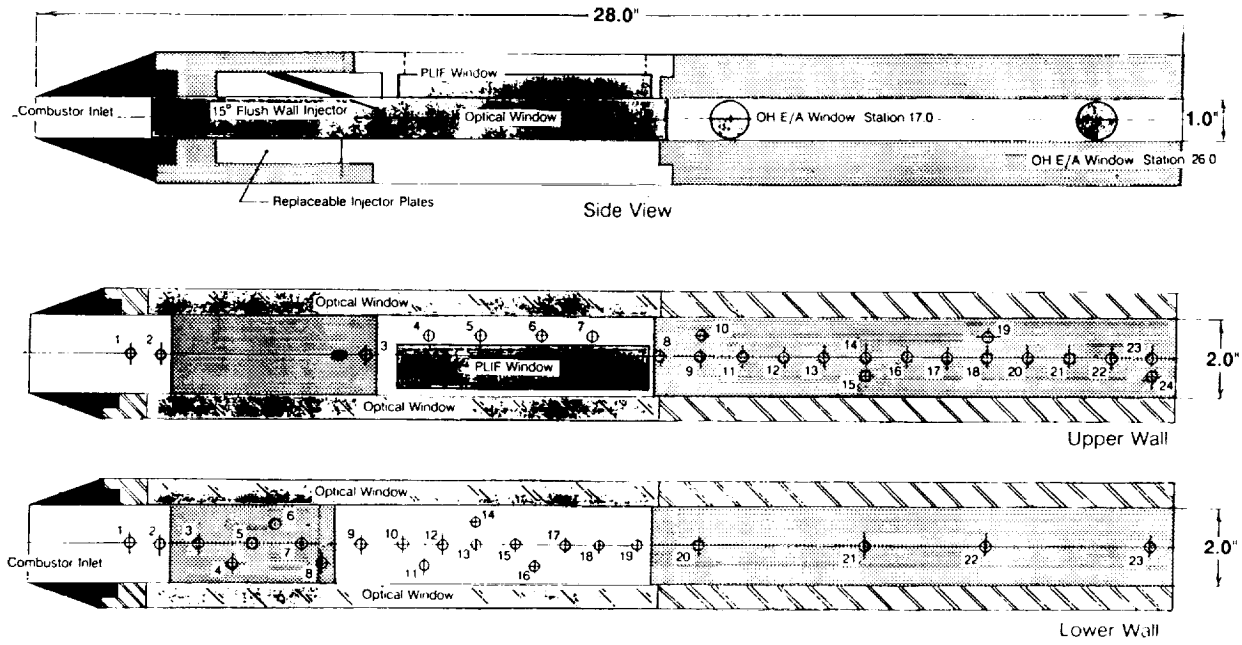

Figure 3. Schematic of combustor model.

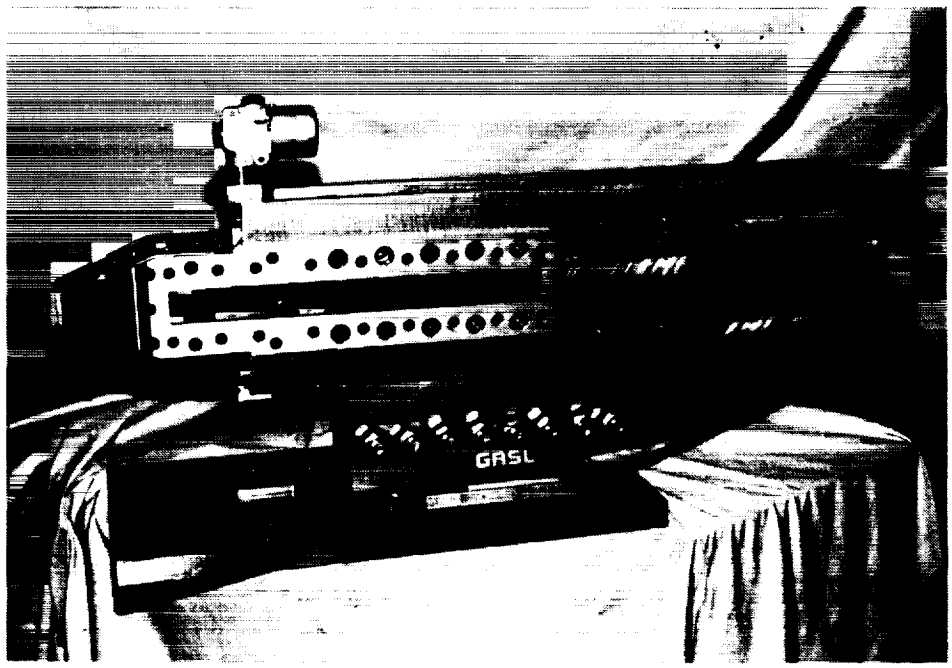

Figure 4. Assembled combustor model.

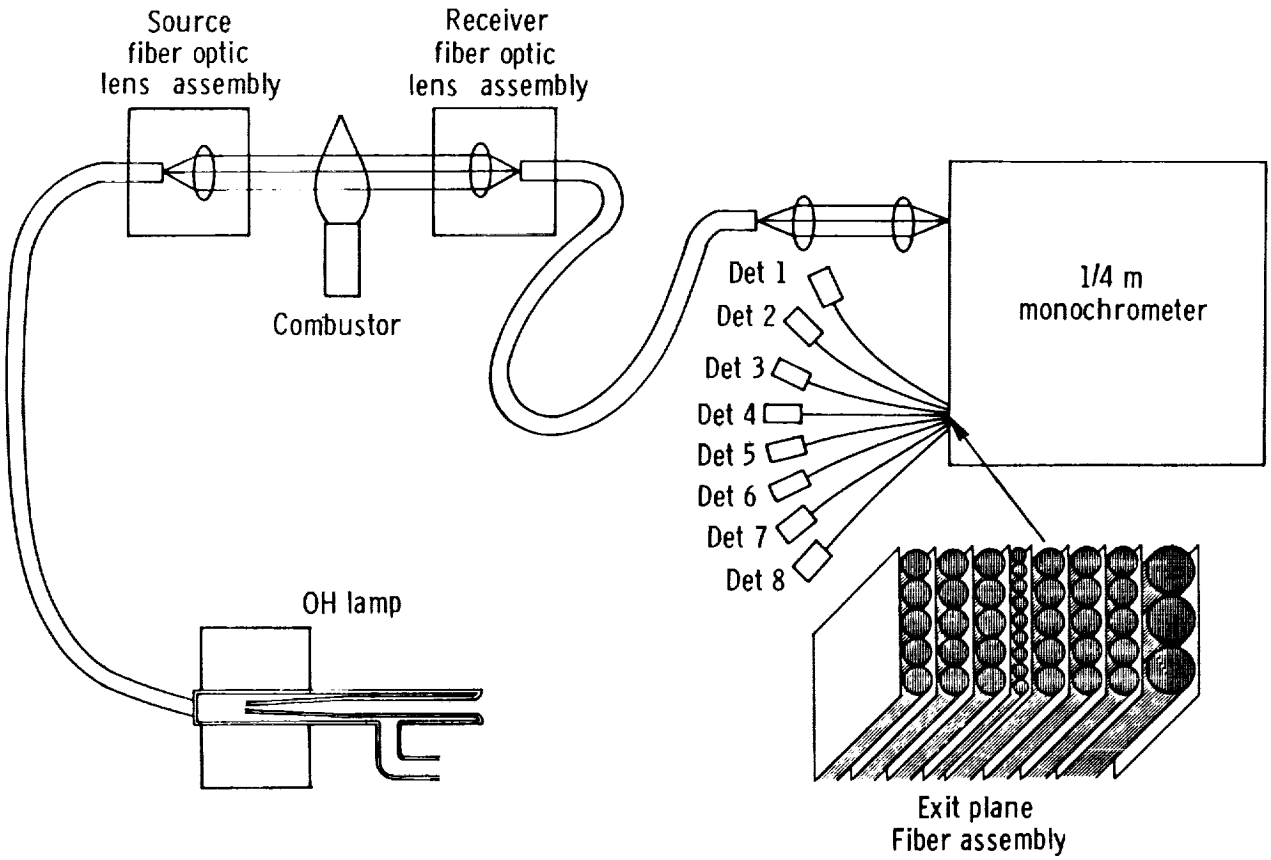

Figure 5. Schematic of resonance lamp absorption apparatus.

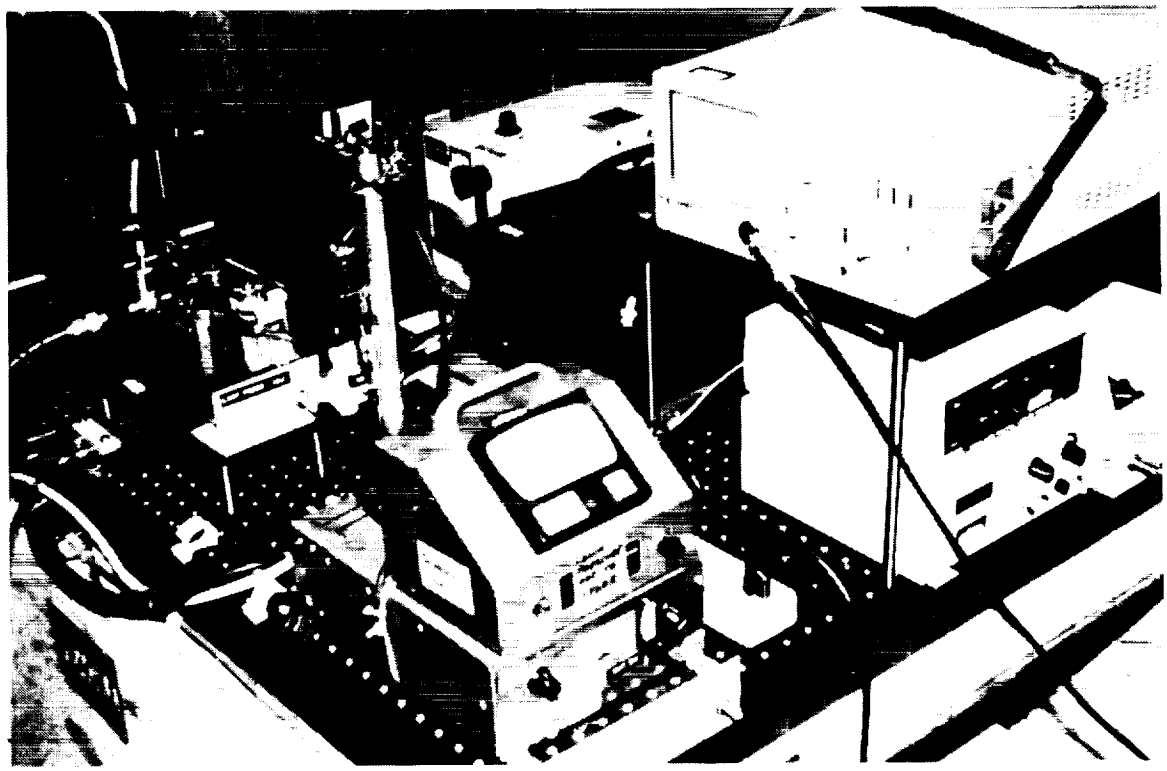

Figure 6. Assembled resonance lamp absorption apparatus.

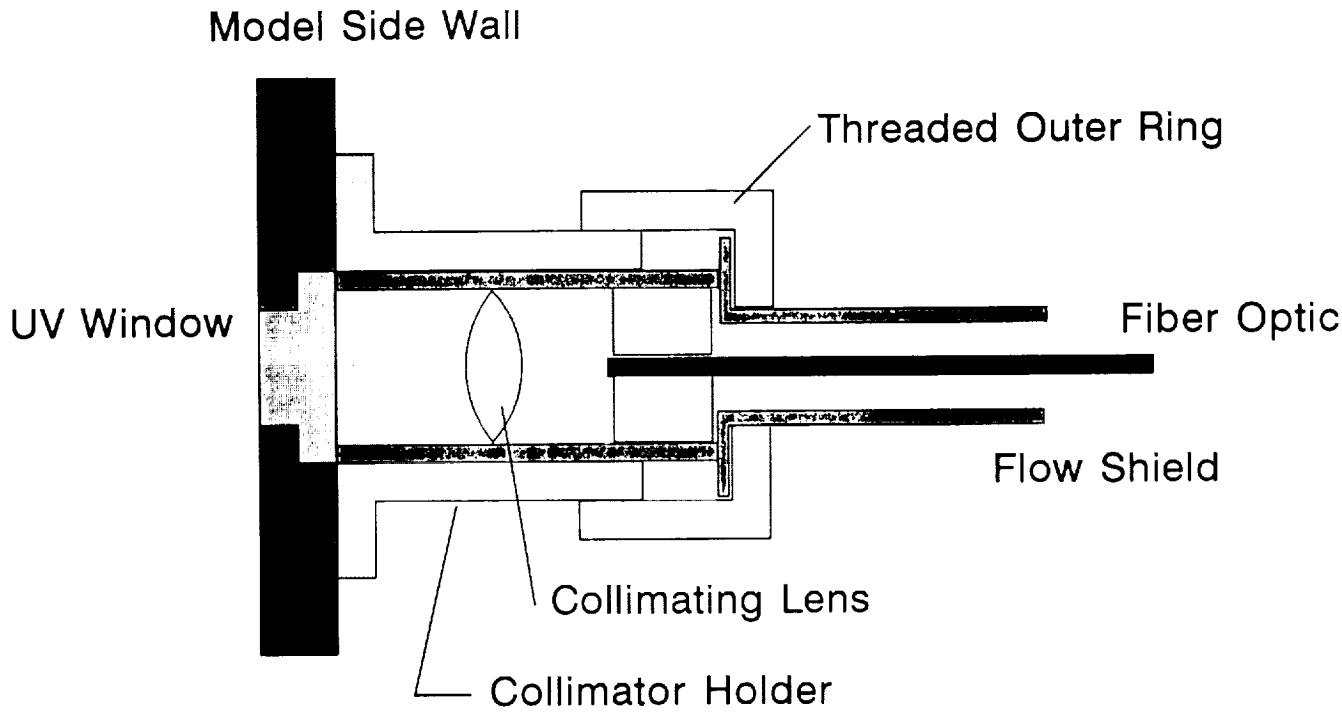

Figure 7. Schematic of optical fiber/model interface.

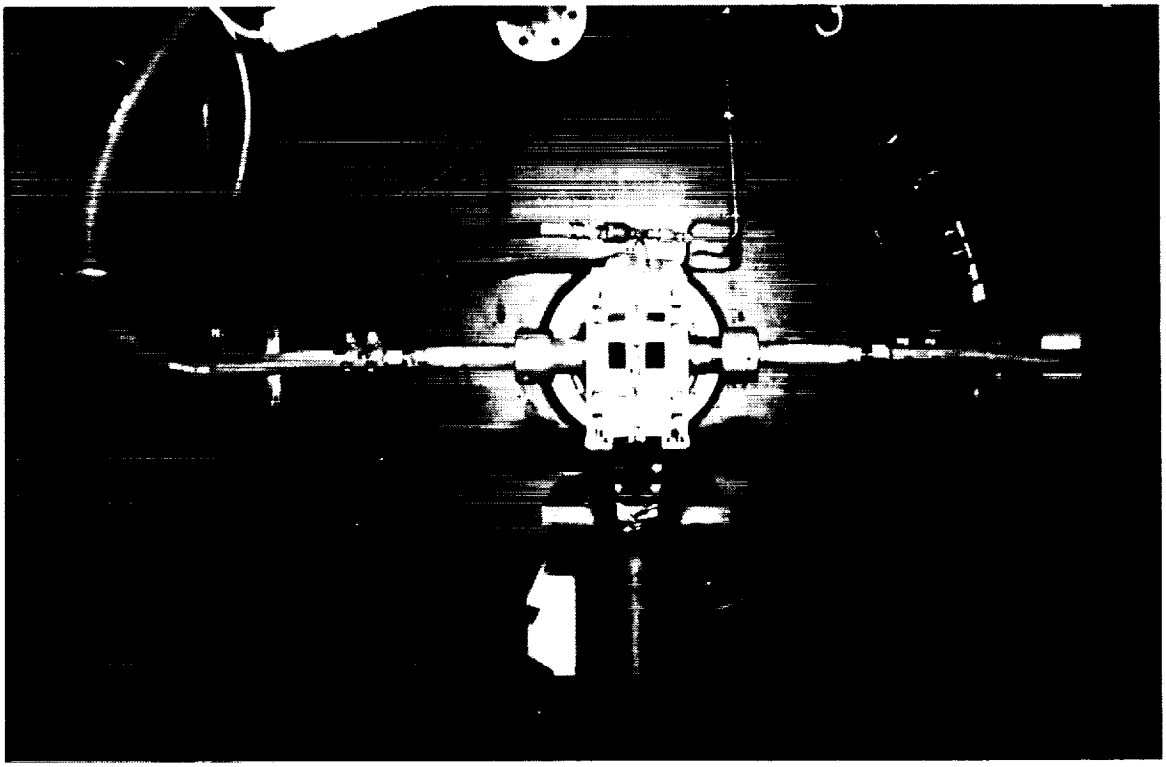

Figure 8. Optical fiber/model assembled inside facility test chamber.

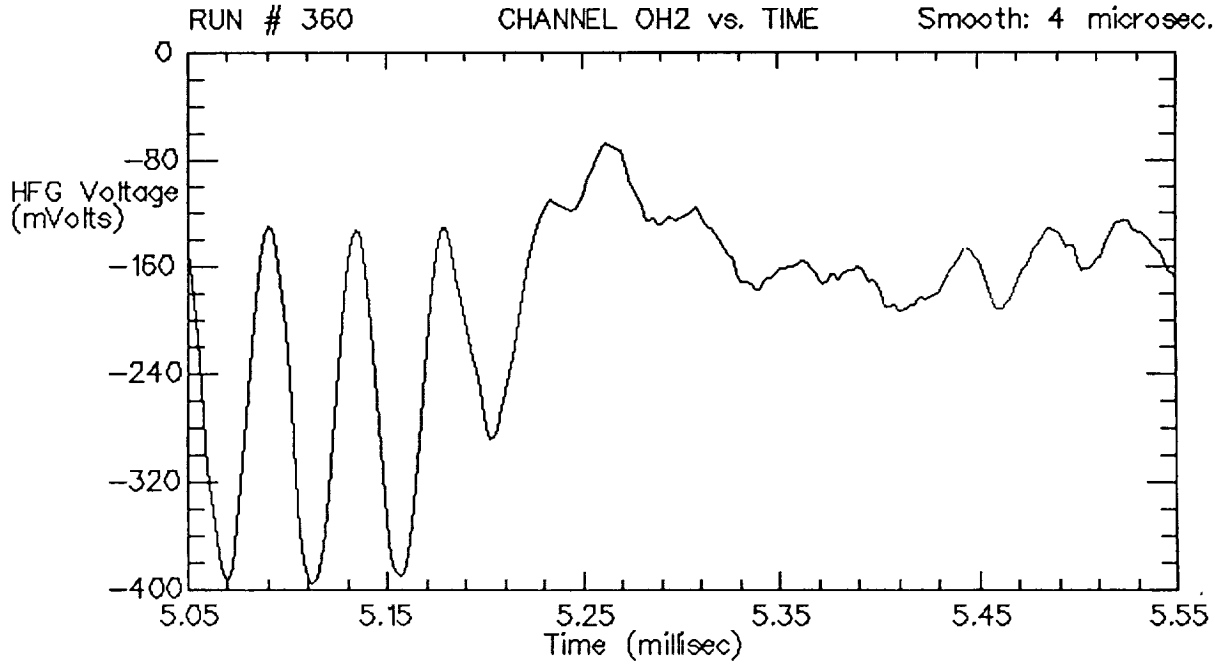

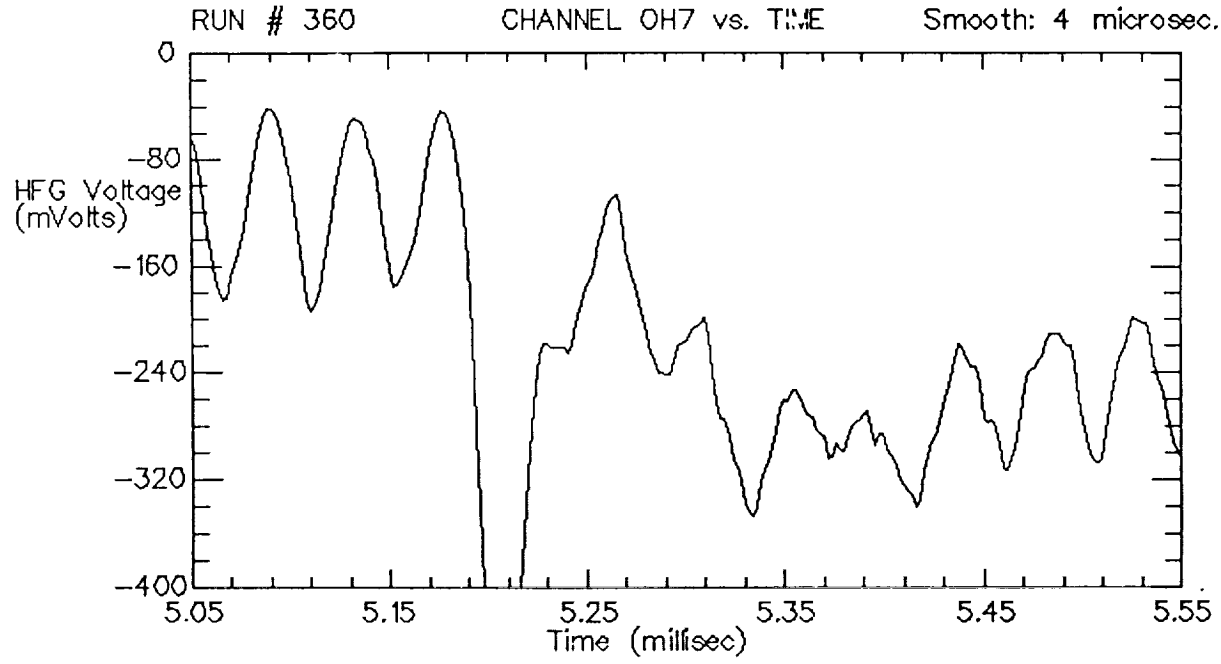

Figure 9. Experimental time traces for OH spectral Channels 2 and 7. ϕ = H_2/O_2 15° flush wall injector test.

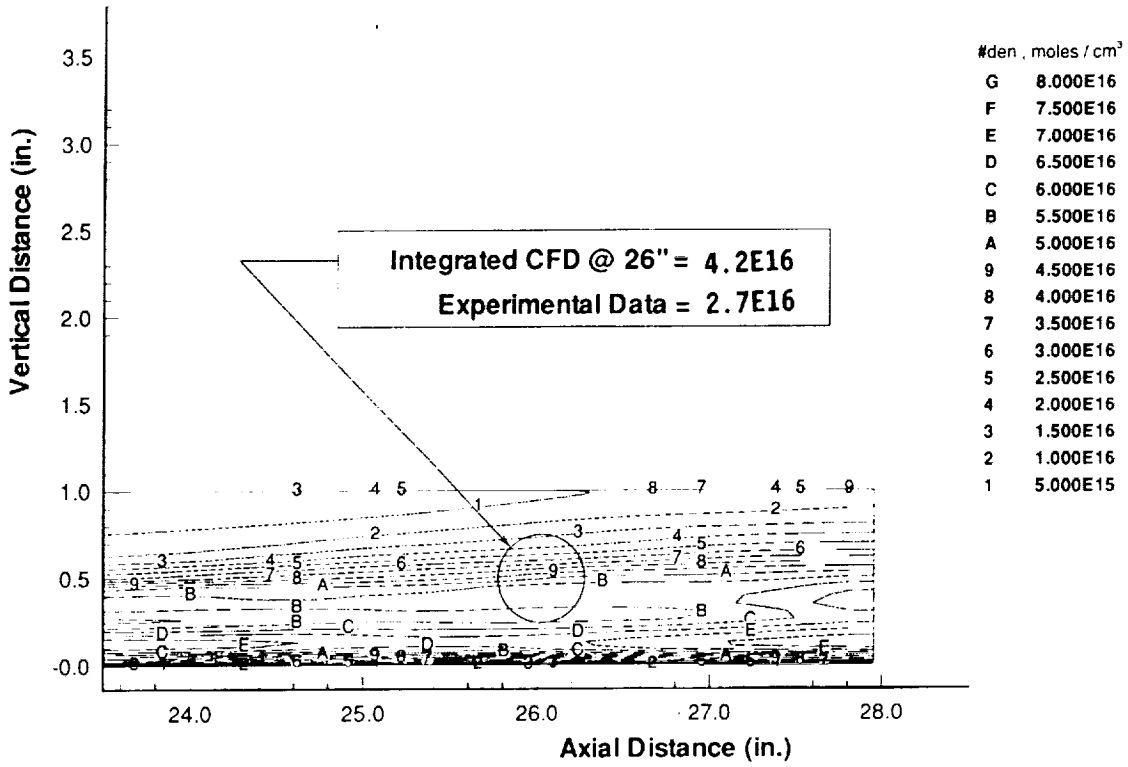

Figure 10. Laterally (Y) averaged contours of OH number density from CFD prediction.

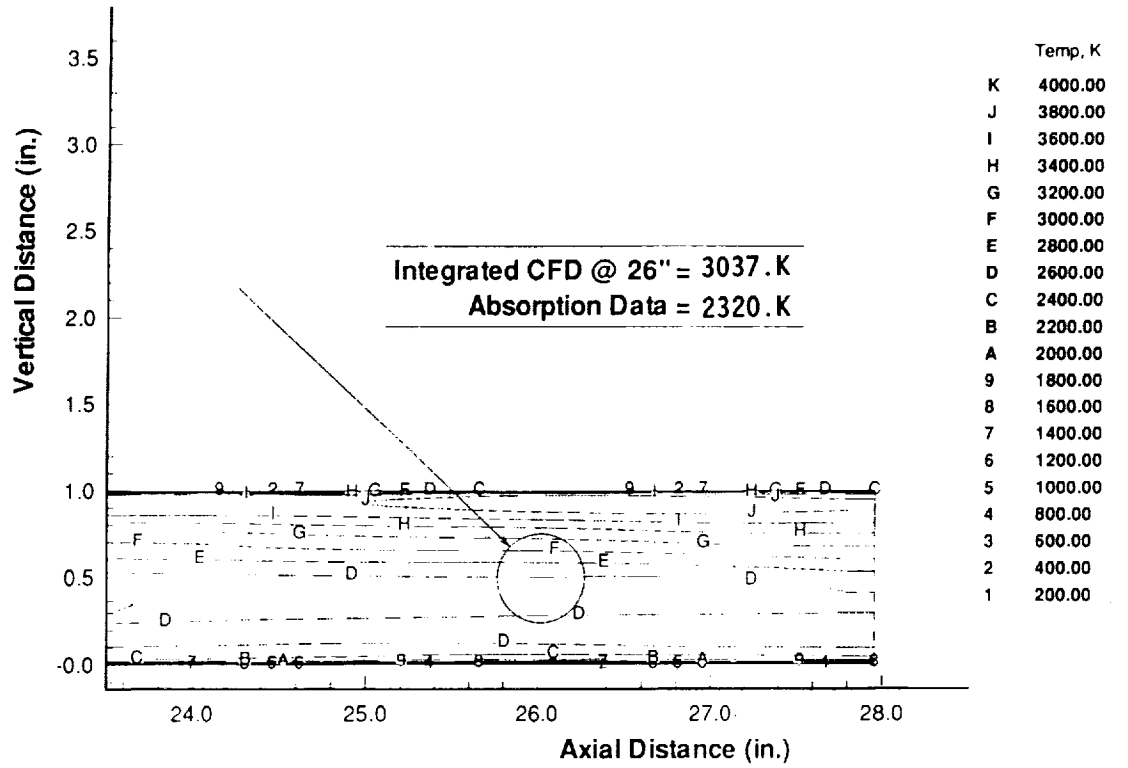

Figure 11. Laterally (Y) averaged contours of static temperature from CFD prediction.